Compact Modeling for a Double Gate MOSFET

21 October 2009

1 Introduction

MOSFETs (metal-oxide-silicon field-effect transistors) are an integral part of modern electronics. Figure 1 shows an outline of a standard MOSFET and also indicates the shrinking of these devices over the last 50 years. Improved designs are currently under investigation, and one that is promising is the double gate MOSFET.

Understanding device characteristics is critical for the design of MOSFETs as part of design tools for integrated circuits such as SPICE. Current methods involve the numerical solution of partial differential equations governing electron transport. A typical example of such a solution is shown in Figure 2. Numerical solutions are accurate, but do not provide an appropriate way to optimize the design of the device, nor are they suitable for use in chip simulation software such as SPICE. As chips contain more and more transistors, this problem will get more and more acute.

There is hence a need for analytic solutions of the equations governing the performance of MOSFETs, even if these are approximate. Almost all solutions in the literature treat the long-channel case (thin devices) for which the PDEs reduce to ODEs. The goal of this problem is to produce analytical solutions based on the underlying PDEs that are rapid to compute (e.g. require solving only a small number of algebraic equations rather than systems of PDEs).

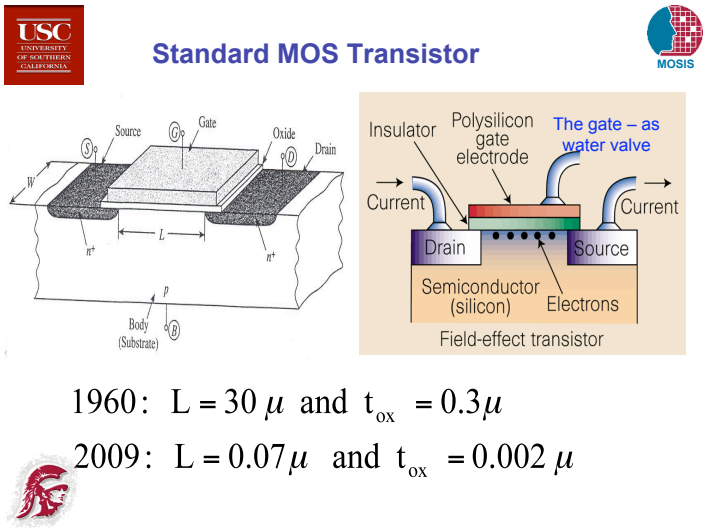

Figure 1: Schematic of MOSFET device.

2 Model

The formulation is presented in Appendix-1. The PDE problem (in dimensionless variables) we consider is

$$2\left(\frac{\partial^2 w}{\partial x^2}+\delta^2\frac{\partial^2 w}{\partial y^2}\right)=\sigma^2 e^{w-\phi}, \tag{1}$$

$$\frac{\partial}{\partial x}\left(e^{w-\phi}\frac{\partial \phi}{\partial x}\right)+\delta^2\frac{\partial}{\partial y}\left(e^{w-\phi}\frac{\partial \phi}{\partial y}\right)=0. \tag{2}$$

The domain is $|x|<1, 0<y<1$, for which the boundary conditions are

$$w=W_{bi}, \qquad \phi=0 \qquad \text{at } y=0, \tag{3}$$

$$w=W_{bi}+V_{ds}, \qquad \phi=V_{ds} \qquad \text{at } y=1, \tag{4}$$

$$\frac{\partial w}{\partial x}=\mp r(w-V_{gs}), \qquad \frac{\partial \phi}{\partial x}=0 \qquad \text{at } x=\pm 1. \tag{5}$$

Then $w(x,y)$ is an even function of x, enabling the more convenient condition

$$\frac{\partial w}{\partial x}=0 \qquad \text{at } x=0, \tag{6}$$

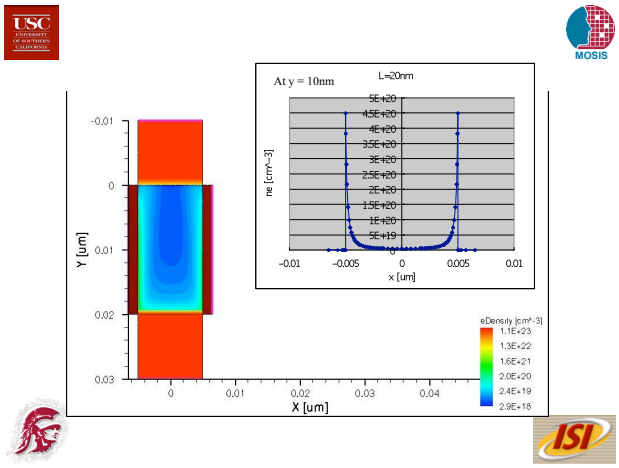

Figure 2: Numerical solution courtesy for the MOSFET device produced by the group of Prof. Uno of Nagoya University. The colored diagram gives the electron density. The curve gives a section of the electron density through the middle of the device.

to be used with $0 < x < 1$. With $0 < y < 1$, the aspect ratio specified in the problem formulation is $\delta = 1/12$. Figure 3 shows the field equations, boundary conditions and geometry.

In this form, the governing equations and boundary conditions are, except for $0 < y < 1$, those in §3 of the MITACS 2007 Simon Fraser report. The solution given by Eq. 11 of MITACS is even in x, which indicates that Eq. 3 and its predecessor should have $\pm$ on their left-hand-sides. The replacement of $w(\pm 1)$ by $w(1)$ in Eq. 3 is consistent with this observation. Physically, the sign of the voltage difference distinguishes between inflow and outflow rather than determines the flow direction.

As in MITACS, the electric and Fermi potentials, w, ϕ, and the voltages W_{bi}, V_{ds}, V_{gs} have been scaled on $V_{th} = kT/q$, the thermal voltage of the system. $\sigma = 2 \times 10^{-4}$ and r is determined from

$$2r = \frac{\text{permittivity ratio, oxide to silicon}}{\text{thickness ratio, oxide to silicon}}.$$

We note that both σ and δ are small.

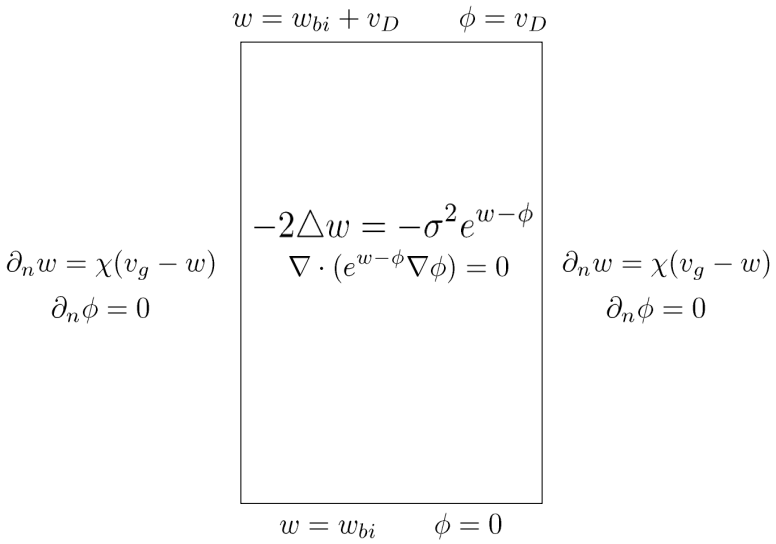

Figure 3: Domain, field equations and boundary conditions.

Such a small value of σ suggests that an approximate solution be constructed by deleting the forcing term in the Poisson equation (1). However, this approach annihilates a significant feature of the electric potential w and hence is not pursued here. The obvious alternative strategy is to neglect terms involving $\delta = 1/12$. Equivalently, for cross channel flow in the bulk of the rectangle, assume x-derivatives of w dominate those with respect to y and note that $\phi = \phi_0(y)$ then satisfies the governing equation for ϕ. (In Chen *et al.* $\phi_0(y)$ is taken to be a delta function). Thus solve

$$2\frac{\partial^2 w_0}{\partial x^2} = \sigma^2 e^{w_0 - \phi_0(y)}. \tag{7}$$

The substitution,

$$w_0(x) - \phi(y) + 2\ln\sigma = W(x), \tag{8}$$

reduces the differential equation (7) to the standard form,

$$2\frac{\partial^2 W}{\partial x^2} = e^W, \tag{9}$$

whose even solution is

$$W(x) = 2\ln[2\theta\sec(x\theta)], \qquad W(0) = 2\ln(2\theta). \tag{10}$$

This reproduces Eq. 11 of MITACS, after correcting a typo. The only relevance of θ to angles is that $0 < \theta < \pi/2$. The parametric dependence of θ on y, determined by applying the condition (5) at $x = 1$, is given by

$$\frac{2}{r}\theta \tan\theta = V_{gs} - \phi_0(y) + 2\ln\left(\frac{\sigma\cos\theta}{2\theta}\right). \tag{11}$$

Evidently a further relation between θ and ϕ_0 is needed (unlike Abebe *et al.* where this is specified in advance). A compatibility condition is established, prior to any approximations and for $\delta > 0$, by integrating (2) with respect to x and using the second of conditions (5. Although the approximation, $\phi \sim \phi_0(y)$ also eliminates the first term of (2), we choose to use the compatibility condition as a convenient way to reduce the governing equation for ϕ_0 to an ODE. On inserting the above $w \sim w_0$ approximation, it follows that

$$\frac{d}{dy}\left[e^{W(0)}\frac{\tan\theta}{\theta}\frac{d\phi_0}{dy}\right] = 0,$$

and hence

$$\theta\tan\theta\frac{d\phi_0}{dy} = A,$$

which MITACS identified as a constant current condition. Substitution of the earlier relation (11) gives a first order differential equation whose integration is elementary and yields

$$Ay = \theta^2 - 2\theta\tan\theta - \frac{\theta^2}{r}\tan^2\theta + B. \tag{12}$$

Although the above construction likely fails near $y = 0$ and $y = 1$, where significant boundary layers of thickness $O(\delta)$ are anticipated, the non-appearance of δ in (11) allows $\theta_0 = \theta(0), \theta_1 = \theta(1)$ to be determined by applying the conditions on ϕ at $y = 0, 1$. Thus, according to (11),

$$\frac{2}{r}\theta_0\tan\theta_0 = V_{gs} + 2\ln\left(\frac{\sigma\cos\theta_0}{2\theta_0}\right),$$

$$\frac{2}{r}\theta_1\tan\theta_1 = V_{gs} - V_{ds} + 2\ln\left(\frac{\sigma\cos\theta_1}{2\theta_1}\right).$$

Estimates are

$$\theta_0 \sim \frac{\pi}{2} - \frac{\pi}{rV_{gs}},$$

$$\theta_1 \sim \begin{cases} \frac{\pi}{2} - \frac{\pi}{r(V_{gs}-V_{ds})} & (V_{gs} \gg V_{ds}) \\ \frac{\sigma}{2}\exp[-(V_{ds}-V_{gs})/2] & (V_{gs} \ll V_{ds}) \end{cases}$$

The constants A, B are then found by setting $y = 0, 1$ in (12) to obtain

$$0 = \theta_0^2 - 2\theta_0 \tan\theta_0 - \frac{\theta_0^2}{r}\tan^2\theta_0 + B,$$

$$A = \theta_1^2 - 2\theta_1 \tan\theta_1 - \frac{\theta_1^2}{r}\tan^2\theta_1 + B.$$

Evidently $\theta(y)$, and hence $\phi_0(y)$, varies little when $V_{gs} \gg V_{ds}$, in which case

$$\theta(y) \sim \frac{\pi}{2} - \frac{\pi}{r(V_{gs} - V_{ds}y)}, \qquad \phi_0(y) \sim V_{ds}y.$$

If $V_{gs} \ll V_{ds}$, then

$$1 - y \sim \frac{\theta^2 - 2\theta\tan\theta - \frac{\theta^2}{r}\tan^2\theta}{\theta_0^2 - 2\theta_0\tan\theta_0 - \frac{\theta_0^2}{r}\tan^2\theta_0}.$$

In general, the parametric dependence of W on y disallows the obvious approximation $\phi \sim V_{ds}y$ but in the former case this dependence is essentially absent. At this stage, it must be borne in mind that only the cross-channel mean of (2) has been used and that $\delta > 0$ is required for its applicability.

The remaining conditions on w at $y = 0, 1$ are not satisfied by w_0 and so a correction w_1 is needed in 'boundary layers' adjacent to these edges. On assuming that y-derivatives of w_1 are sufficiently dominant and $|w_1| \ll 1$, the governing equation for w gives

$$2\delta^2 \frac{\partial^2 w_1}{\partial y^2} = \sigma^2 e^{w_0 - \phi_0(y)} w_1 \sim \sigma^2 e^{W_{bi}} w_1, \tag{13}$$

near $y = 0, 1$. Hence w_1 exhibits exponential decay away from $y = 0, 1$ on the scale $\sqrt{2e^{-W_{bi}}}(\delta/\sigma)$ in each layer.

3 Results

To examine the accuracy of the analytical model of § 2, its predictions were compared with numerical simulations carried out by Prof. Uno and also with

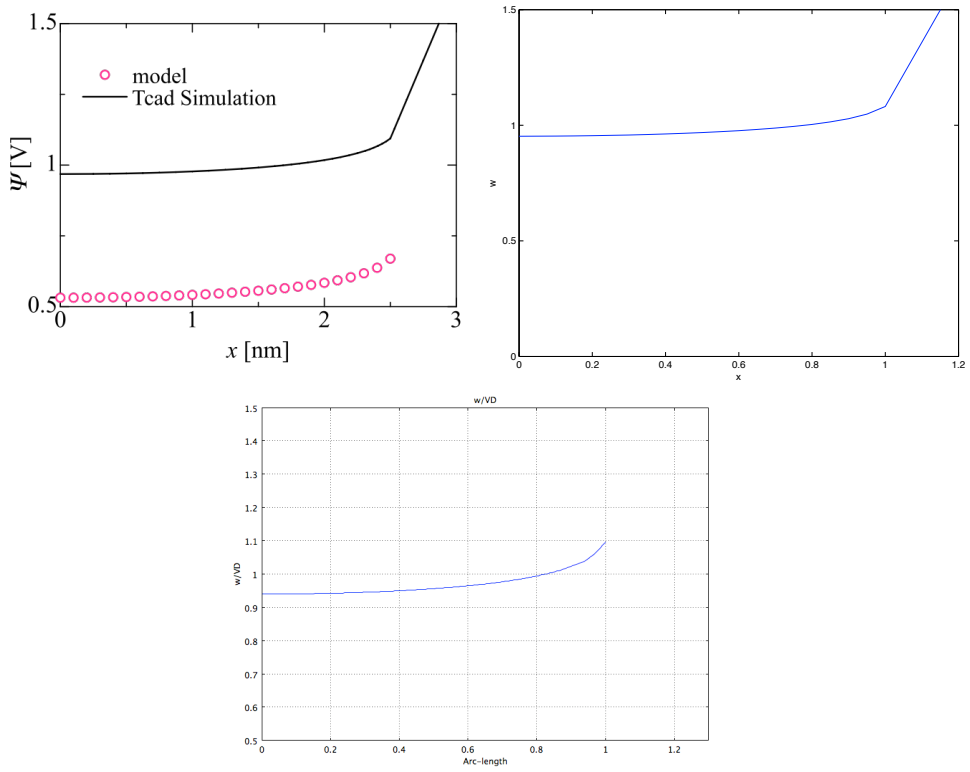

Figure 4: (a) Potential in middle of device calculated by Prof. Uno. (b) Analytic prediction. (c) FEMLAB calculation.

FEMLAB calculations carried out during the workshop. Two sets of parameter values were used. The first used the MITACS parameter values, except with $t_{ox} = 1.5 \times 10^{-9}$ m, $V_g = 2.75$ V and $V_D = 1$ V. Figure 4 shows the electrostatic potential at the midpoint of the device for all three calculations. The agreement is excellent. Note that the analytical model requires solving two nonlinear equations for θ_0 and θ_1 and some interpolation, and is hence extremely fast. Further details of the solution are shown in Figure 5. The Fermi potential $\phi_0(y)$ is nearly linear in this limit of large gate potential.

The second set of parameter values corresponds to a subcritical regime and is shown in Figure 6. In this case $V_g = 0.37$ V, $V_D = 2$ V, $t_{ox} = 1.6 \times 10^{-9}$ V and the channel is shorter: $\delta = 1/8$. Now the Fermi potential is no longer linear and the total electron density no longer has structure across

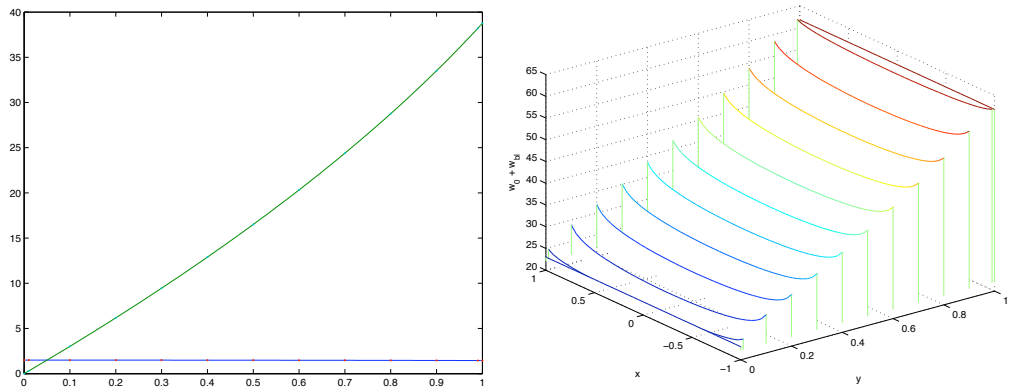

Figure 5: (a) Fermi potential $\phi_0(y)$ (green curve) and auxiliary variable $\theta(y)$ (blue curve). (b) Electron density in device $w(x, y)$ incorporating boundary-layer correction (13).

the channel.

4 Conclusions

Guided by asymptotic analysis, a fast numerical procedure has been developed to obtain approximate solutions of the governing PDES governing MOSFET properties, namely electron density, Fermi potential and electrostatic potential. The approach depends on the channel's being long enough, and appears accurate in this limit.

References

Physical Models of a Double Gate MOSFET. *MITACS Industrial Summer School 2007, Simon Fraser University.*

Chen, Q., Harrell, E. M. and Meindl, J. D. 2003 A physical short-channel threshold model for undoped symmetric double-gate MOSFETs. *IEEE Trans. Electron Dev.*, **50**, 1631–1637.

Abebe, H., Cumberbatch, E., Morris, H. and Uno, S. Compact models for double gate and surround gate MOSFETS.

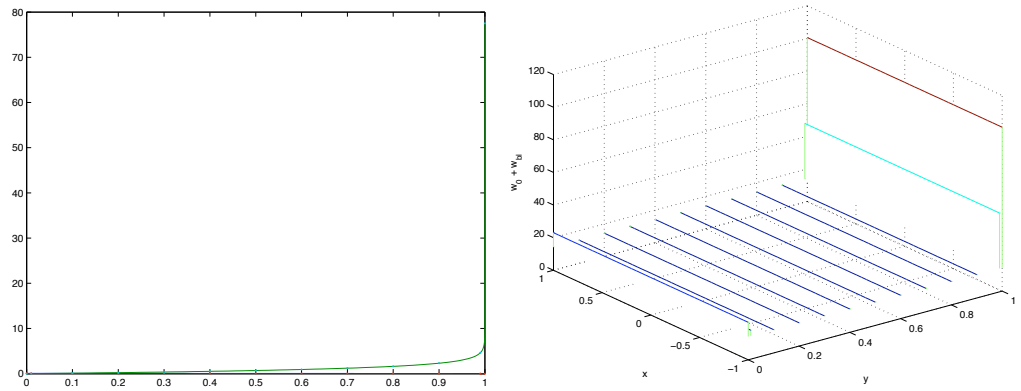

Figure 6: (a) Fermi potential $\phi_0(y)$ (green curve) and auxiliary variable $\theta(y)$ (blue curve). (b) Electron density in device $w(x, y)$ incorporating boundary-layer correction (13).

Contributors

Henok Abebe, Information Sciences Institute
Saleem Ahmed, SUNY at Buffalo
Chris Breward, University of Oxford
Darren Crowdy, California Institute of Technology
Ellis Cumberbatch, Claremont Graduate University
Anthony Davis, UC San Diego
Joseph D. Fehribach, Worcester Polytechnic Institute
Mike Grigsby, Cal Poly Pomona
Cameron Hall, University of Oxford
Stefan Llewellyn Smith, UC San Diego

Appendix-1

Compact Modeling for a Double Gate MOSFET. Henok Abebe and Ellis Cumberbatch

Henok Abebe is a Senior Member of IEEE and works at MOSIS Service. (See http://www.isi.edu/~abebeh/)
MOSIS is a low-cost prototyping and small-volume production service for VLSI circuit development. Since 1981, MOSIS has fabricated more than 50,000 circuit designs for commercial companies, government agencies, and research and educational institutions around the world [1].

A compact, physical, potential model for undoped (or slightly doped) short-channel Double Gate (DG) MOSFETs is required.

1 Introduction

Most transistors go by the name of MOSFET (metal-oxide-silicon field-effect transistor). The current design has various features that are proving undesirable as technology mandates the endless reduction in transistor size. There is extensive research and development underway with new designs. One which looks favourable is the double gate (DG MOSFET). Current methods of determining device characteristics for a single transistor include numerical solutions of the partial differential equations governing electron transport. (Quantum effects are now important, but this aspect is not intended for this workshop.) While numerical treatments are satisfactory in providing accurate results, they do not provide a framework for analyzing device parameter optimization. This becomes increasingly important as the scale of the devices drops to the nanoscale regime, and as the number of material parameters increases. Additionally, the time consumption of numerical solutions often precludes their use in SPICE, the simulation software used to obtain chip performance, when the chip contains many transistors. (This number can now approach 1 billion.)
Almost all the analytical solutions for DG MOSFETs in the literature treat the long-channel case ($L >> T_{si}$) for which the PDEs reduce to ODEs, and there is a scarcity of solutions in the short-channel (PDE based) case. An analytical, physically based PDE model (or at least a model that is extremely fast numerically) would allow determination of optimal parameters for device performance, allow a reduction of the amount of time to determine device characteristics, and be available for use in SPICE.

2 Introduction to MOSFETS

The device comprises: a silicon wafer on which an oxide (SiO2) and a metal gate (or a polysilicon region) is deposited. Metal contacts are deposited at the source and drain. Positive voltage at the gate(s) generates large electron densities in the silicon, and current flow source-to-drain is achieved by a difference in voltage at those contacts. The DG MOSFET, is a new geometry in which a second gate is added. This design helps reduce short-channel interference effects and increase the performance of the device.

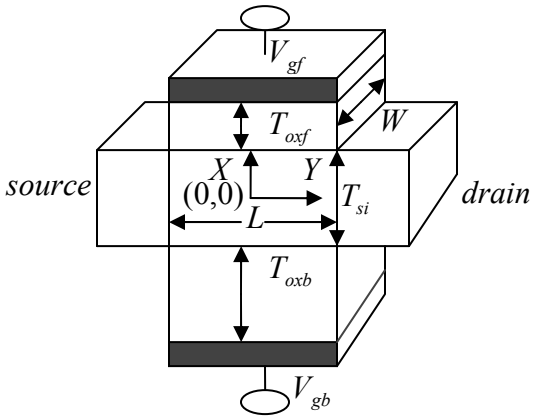

Figure 1: Schematic diagram of a typical DG MOSFET illustrating device dimensions and model coordinates centered in the MOSFET silicon bulk.

A current design of the DG MOSFET is shown in Figure 1. DG MOSFETs are of great interest due to their potential as a replacement for standard planar MOSFETs. Double gate devices possess more current efficiency over planar devices of similar length scales as their design eliminates the need for a bulk region of carriers. DG MOSFETs are lightly doped which means, for modeling, that the electron density in the silicon body is well above the doping density, and the latter may be neglected. There is then no depletion region and no free boundary problem to solve.

A substantial number of long-channel solutions are available [e.g. 2, 3 and 4]. We shall describe the character of these subsequently as they may be useful in formulating a short-channel approximation, required when the channel length approaches the sub-65nm range. A well quoted paper by Chen et al., [2], attempts such a 2-D solution for the case of devices in near-equilibrium. In this "threshold" scenario, the distribution of electrons in the silicon is relatively constant, allowing a linearization about this solution.

Recently we developed an approximate solution based on assuming a quadratic electrostatic potential across the device, see [5]. This approach gives good accuracy for *symmetric* devices in all regions. However, its accuracy for *asymmetric* device deteriorates rapidly in the weak inversion and saturation regions.

3 Drift-Diffusion Physics

The electron number density is denoted by n and the electron current flux is assumed to be the sum of a diffusion term plus a drift term linear in $\overline{E} = -\nabla\psi$, the electric field. This gives

$$\bar{J} = (J_X, J_Y) = qn\mu_n \nabla(-\psi + \frac{kT}{q}\ln(n)) = qn\mu_n \nabla\varphi_n \qquad (1)$$

for the electron current flux, where q is the charge on an electron and n is the number density of electrons. In (1), the Einstein relation $D=kT\mu_n/q$ between the electron mobility μ_n and the diffusion coefficient D has been used. (k is Boltzmann's constant and T is the temperature.) The last part of (1) defines the quasi-Fermi potential φ_n. With this definition the electron density can be expressed as $n = n_i e^{(\psi-\varphi_n)/V_{th}}$ where n_i is a constant known as the intrinsic electron density ($n_i \sim 10^{16} m^{-3}$) and where

$$V_{th}=kT/q \tag{2}$$

is known as the thermal voltage. For our applications V_{th}=0.0259 volts, so that changes in potential of 1 volt give rise to factors multiplying n by $exp(38.6)$.

Gauss's Law is $\nabla \cdot \overline{D} = \rho = -qn$

where $\overline{D} = \varepsilon \overline{E}$, is the electric displacement field and ρ is the total charge density, given in this model by the electron charge only.

Conservation of current: This is given by $\nabla \cdot \overline{J} = 0$

Since no current crosses the insulating gate boundaries the current is constant crossing any plane Y constant. This current may be expressed as

$$I = W \int_{-\frac{T_{si}}{2}}^{\frac{T_{si}}{2}} J_Y dX \tag{3}$$

Boundary Conditions (refer to Figure 1). The potential and the displacement field are both continuous across the oxide-silicon interfaces. The oxide films have zero charge and are thin so the potentials across them may be considered linear in the X-direction. This means that the (*Robin*) boundary conditions at the two interfaces are

$$\varepsilon_{si} \left.\frac{\partial \psi}{\partial X}\right|_{X=\frac{T_s}{2}} = \varepsilon_{ox}\left(\frac{V_{gf} - \psi_{sf} - \Delta\phi}{T_{oxf}}\right), \varepsilon_{si} \left.\frac{\partial \psi}{\partial X}\right|_{X=\frac{-T_s}{2}} = -\varepsilon_{ox}\left(\frac{V_{gb} - \psi_{sb} - \Delta\phi}{T_{oxb}}\right) \tag{4}$$

where ψ_{sf}, ψ_{sb} represent the potentials at $X = \pm T_{si}/2$ and where the gate-source voltages applied at each gate is reduced by the difference in work functions $\Delta\phi$ between the gate and semi-conductor materials. The conditions at the source and drain ends of the channel are determined by the built-in voltages between the p-n junctions of the source or drain and the silicon supplemented by the voltage difference applied.

4 Non-Dimensionalization

Device lengths, potentials and voltages are scaled as follows for the 2-D problem (no variation is considered in the third dimension).

$$(X,T_{ox})=\frac{T_{si}}{2}(x,t_{ox}),\ Y=Ly,(\psi,\varphi_n)=V_{th}(w,\varphi),\ L_D^2=\frac{V_{th}\varepsilon_{si}}{2qn_i},\ \delta=T_{si}/L \text{ and } \sigma=\frac{T_{si}}{2\sqrt{2}L_D} \quad (5)$$

For a typical case T_{si}=10nm, L=60nm, L_D=24 microns, δ=1/12 and $\sigma=1.4\times10^{-4}$. In terms of non-dimensional quantities the PDE system may now be written as

$$2\{\frac{\partial^2}{\partial x^2}+\delta^2\frac{\partial^2}{\partial y^2}\}w=\sigma^2\exp[(w-\varphi)] \quad (6)$$

$$\frac{\partial}{\partial x}(e^{w-\phi}\frac{\partial\phi}{\partial x})+\delta^2\frac{\partial}{\partial y}(e^{w-\phi}\frac{\partial\phi}{\partial y})=0 \quad (7)$$

with δ and σ small, and boundary conditions given on a rectangle $|x|<1,0<y<1$.

5 The quasi-1-D or Long-Channel Approximation

For $T_{si}/L=\delta\rightarrow 0$ the y derivatives in (6) may be neglected. In addition it can be shown that φ is a function of y only so that (7) becomes an ODE. For the symmetric case in which the gate conditions are identical the 1-D Poisson equation for undoped symmetric DG-MOSFET is

$$\frac{d^2\psi}{dX^2}=\frac{q}{\varepsilon_s}\left(n_i e^{q(\psi-\phi)/kT}\right) \quad (8)$$

In scaled variables (8) becomes

$$2\frac{d^2w}{dx^2}=e^{(w-\varphi)} \quad (9)$$

with the different scaling: $(\psi,\phi)=(w,\varphi)V_{th},\ X=xL_D$

In (9), w,φ are the scaled electrostatic and quasi-Fermi potentials, respectively, with φ being dependent only on the source-to-drain coordinate, y. The solution to (9) in the symmetric case is:

$$w(x)=v+w_0-2\ln(\cos(e^{w_0/2}x/2)) \quad (10)$$

where w_0 represents the minimum value of w at $x=0$. The boundary condition at the oxide/silicon interface yields the transcendental equation for θ:

$$v_{gs}-\Delta\varphi-v=2\ln(c_1\theta\sec(\theta))+c_2\theta\tan(\theta) \quad (11)$$

where v_{gs} is the scaled gate voltage and θ,c_1,c_2 are defined by $\theta=\frac{1}{4}e^{w_0/2}t_{si}$, $c_1=4\frac{L_d}{T_{si}}$, $c_2=4\frac{\varepsilon_s}{\varepsilon_{ox}}\frac{T_{ox}}{T_{si}}$.

A short-channel model of this type has been explored in [2], however, solutions outlined are valid only at near-threshold voltage operations. In practical use, large variations in V_{gs} are applied to the device and model developments for the non-equilibrium device functions are of great importance.

References

[1] MOSIS Service, URL: http://www.mosis.com

[2] Q. Chen, E. Harrell, and D. Meindl. A Physical Short-Channel Threshold Voltage Model for Undoped Symmetric Double-Gate MOSFETs. IEEE Transactions on Electron Devices, 50(7), July 2003.

[3] H. Lu and Y. Taur. Physics-Based, Non-Charge-Sheet Compact Modeling of Double Gate MOSFETs. Presented at Nanotech 2005.

[4] Y. Taur, X. Liang, W. Wang, and H. Lu. A continuous, analytic drain-current model for DG MOSFETs. Electron Device Letters, IEEE, 25(2):107–109, 2004.

[5] H. Abebe, E. Cumberbatch, H. Morris and V. Tyree. Asymmetric Double Gate MOSFET Compact Model. Presented at MOS-AK meeting in San Francisco, December 13, 2008 (URL: http://www.mos-ak.org/sanfancisco/)

Appendix-2

Mathematical Facts (may not be useful for practical application).

Solution to $\nabla^2 w = \frac{-\alpha}{2} e^{\beta w}$ is,

$$w = \frac{-2}{\beta} \ln\left\{\sqrt{|\alpha|\beta^2}\,[1 + sign(\alpha\beta)\phi(z)\bar{\phi}(z)/4|\phi'(z)|]\right\} \qquad (12)$$

For any analytic function ϕ of $z=x+iy$. Note: This is slightly amended version of solution given in *Polyanin* and *Zaitsev, Hand Book of Non Linear Partial Differential Equations*.